Strain effect on graphene nanoribbon carrier statistic in the presence of non-parabolic band structure*

N A Izuani Che Rosid[1], M T Ahmadi[1,2], and Razali Ismail[1,†]

[1] Department of Electronics and Computer Engineering, Faculty of Electrical Engineering, Universiti Teknologi Malaysia, Skudai 81310, Malaysia
[2] Nanoelectronic Group, Physics Department, Faculty of Science, Urmia University, Urmia 57147, Iran

(Received 14 December 2015; revised manuscript received 15 April 2016; published online 19 July 2016)

The effect of tensile uniaxial strain on the non-parabolic electronic band structure of armchair graphene nanoribbon (AGNR) is investigated. In addition, the density of states and the carrier statistic based on the tight-binding Hamiltonian are modeled analytically. It is found that the property of AGNR in the non-parabolic band region is varied by the strain. The tunable energy band gap in AGNR upon strain at the minimum energy is described for each of n-AGNR families in the non-parabolic approximation. The behavior of AGNR in the presence of strain is attributed to the breakable AGNR electronic band structure, which varies the physical properties from its normality. The linear relation between the energy gap and the electrical properties is featured to further explain the characteristic of the deformed AGNR upon strain.

Keywords: strain graphene nanoribbon, uniaxial strain, current–voltage characteristic

PACS: 68.65.Pq, 61.46.Np, 61.48.–c, 61.48.De **DOI:** 10.1088/1674-1056/25/9/096802

1. Introduction

Nowadays, non-silicon material has gained a great deal of interest among researchers to develop new structures for future nanoelectronics. Graphene is especially believed to overcome the limitation in the silicon technology and takes all of the considerations of making a good transistor. Physically, graphene refers to the two-dimensional (2D) crystal originated from a single sheet of sp^2 carbon atoms.[1] Despite its surprising features such as high mobility and high Fermi velocity, graphene is one of the best gapless materials whose energy band is intersecting near the edges of the Brillouin zone.[2–4] The absence of an energy gap in graphene has been seen as something crucial and rather complex to realize its application for future FET. Instead of two-dimensional graphene, sub-10 nm width graphene stripes called graphene nanoribbons (GNRs) with both zigzag (ZGNR) and armchair (AGNR) edge configurations are one-dimensional by behavior.[5–7] It has been revealed by theoretical calculations that AGNR and ZGNR are both semiconductors,[8] however the appearance of a band gap in AGNR is due to the quantum confinement and edge effects while the band gap in ZGNR is a consequence of the sub-lattice potential variation.[9] As we focus on the graphene structure with sub 10 nm width which highlights the quantum confinement effect on the width direction, the AGNR family is considered. Unlike 2D-graphene, the lateral confinement in GNRs introduces an energy gap close to the Fermi level for AGNRs of $3m$ and $3m+1$ width, while $3m+2$ AGNRs remain metallic. It is not easy to obtain an appropriate energy gap in AGNR since the gap strongly depends on the crystallographic direction of the ribbon axis and the family width. The 1–2 nm width GNR can open up a suitable energy gap usable for the FET channel.[10,11] However, ultra-narrow GNRs ($\geq$ 2 nm) with smooth edges are not easy to be formed while wider AGNR's ribbon width contributes to the smaller energy gap splits. So, it is desirable to alter the GNR for high performance applications. Most recently, applying a strain to the base-transistor material has become a trend in the semiconductor industry. The strain potentially alters the band gap and helps improve the mobility of the charge carrier in the channel, hence boosting the device performance in silicon technology.[12] The same intention has been studied in carbon nanotubes (CNT). It is remarkable to open up a band gap in a metallic CNT and modify the band gap in a semiconductor CNT.[13] Theoretical and experimental studies conducted by a few researchers have found the unique behavior dependences on AGNR width upon strain. The electronic band structure was demonstrated in a zigzag pattern for all three groups of AGNRs,[14,15] while the carrier statistic behaved linearly with the band structure alteration by strain.[16] Additionally, the strain effect on GNR has been explored by scanning tunnelling microscopy,[17] furthermore its effects on the GNR electronic and optical properties have been explored.[18,19] Even though there are several works that have been done pertaining to strain AGNR, the observation on its properties is still lacking.[20] Therefore, modelling and simulations are provided in this paper primarily to observe the effect of the uniaxial strain on AGNR.

*Project supported by the Ministry of Higher Education (MOHE), Malaysia under the Fundamental Research Grant Scheme (FRGS) (Grant No. Q.J130000.7823.4F477). We also thank the Research Management Center (RMC) of Universiti Teknologi Malaysia (UTM) for providing an excellent research environment.

†Corresponding author. E-mail: razali@fke.utm.my

© 2016 Chinese Physical Society and IOP Publishing Ltd

2. Strained graphene nanoribbon model

In this work, AGNR is assumed to be tensile under a smaller uniaxial strain, as shown in Fig. 1. In the presence of the strain, bond lengths R_1, R_2, and R_3 between carbon atoms are expanded and scaled up according to the percentage of strain ε. The change of the hopping parameter t attributed to the bond length variation is remarkable in tuning AGNR sub band structure. It can be defined as a changing in the lattice parameter variable.

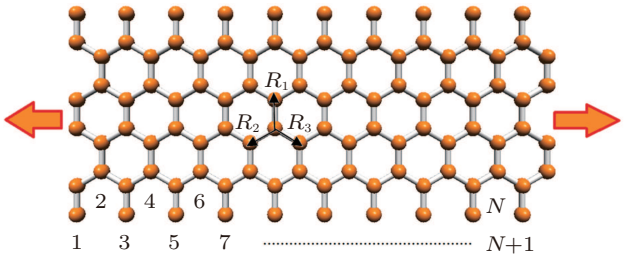


Fig. 1. (color online) AGNR under tensile uniaxial strain.

The sub band structure model plays an important role in predicting the property of quasi one-dimensional (Q1D) strain AGNR. In the Q1D material, the carriers are confined in two directions which are the y and z directions. The carriers are allowed to move in the x direction along the length of the nanoribbon, L_x.

It is well known that the energy $E(k)$ and bandgap in semiconducting AGNR are functions of the AGNR width and can be modelled using either non-parabolic or parabolic approximation as shown in Fig. 2.

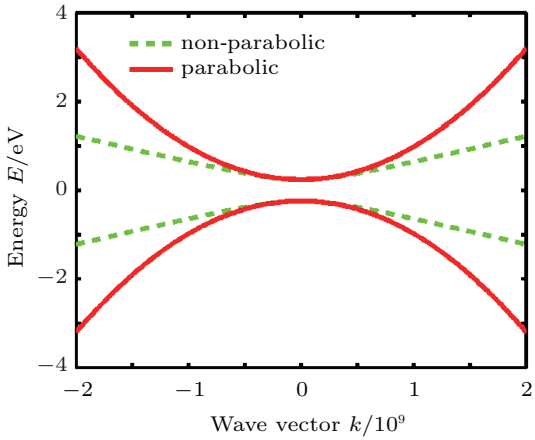


Fig. 2. (color online) The energy dispersion relation of AGNR in the parabolic and non-parabolic band structures near the Fermi point.

For the AGNR at $k = 0$, the band structure is parabolic for both approaches, however the approximation is different for the range out of the parabolic regime. In all circumstances, the non-parabolic approximation is valid to describe all the physical phenomena for AGNR in various energy ranges. By considering an energy level near one of the valleys in the band structure, the energy dispersion relation near the Fermi level in the non-parabolic approximation can be expressed as

$$E(n,k) = \pm\left[t_1^2 + 4t_2^2\cos^2\left(\frac{p\pi}{n+1}\right) + 4t_1t_2\cos\left(\frac{p\pi}{n+1}\right)\cos\frac{3}{2}k_xa\right]^{1/2}, \quad (1)$$

where t_1 and t_2 are the deformed hopping parameters that have been altered by the uniaxial strain as listed in Table 1.[15]

Table 1. Strained AGNR deformed parameters.[15]

Parameter	Value/eV
t_0	2.7
t_1	$t_0/(1+\varepsilon)^2$
$t_2 = t_3$	$t_0/(1+\varepsilon/4)$

The parameters represent the deformed bond length and lattice vectors after the application of the strain. The numbers of dimer lines, n, for three groups of AGNRs are $3m$, $3m+1$, and $3m+2$, and the sub band indices, p, are determined as $2m+1$, $2m+1$, and $2m+2$, respectively, where m is an integer. The k_x represents the wave vector component in the $-x$ direction which is quantized by the periodic boundary condition. By using the Taylor series expansion function, equation (1) can be simplified to

$$E(k_x) = \pm\sqrt{E_c^2 + Bk_x^2}, \quad (2)$$

where the energy band gap E_c and parameter B are given by[15]

$$E_c = \frac{E_g}{2} = 2\left|t_1 + 2t_2\cos\left(\frac{p\pi}{n+1}\right)\right|,$$
$$B = -\frac{9}{2}t_1t_2\cos\left(\frac{p\pi}{n+1}\right)a^2. \quad (3)$$

The conduction and valence bands in the electronic band structure of AGNR exhibit a symmetrical structure as indicated by the $\pm$ sign. Figure 3 shows the energy gap openings close to the Fermi level for $3m$, $3m+1$, and $3m+2$ AGNRs under tensile uniaxial strain. Zigzag and armchair GNRs show metallic and semiconducting properties, respectively. The armchair ribbon is semiconducting when the dimer line number is $N = 3p$ or $N = 3p+1$, however for $N = 3p+2$, it behaves like a semimetal material (p is an integer).[21–23]

It can be observed from the plot that the energy gap splits out linearly for $3m$ and $3m+2$ AGNRs in the same family (Figs. 3(a) and 3(c)), while it decreases and increases linearly in $3m+1$ AGNR (Fig. 3(b)). It is noted from the graph that the band structure of each AGNR family responds differently upon strain. This variation is caused by the different quantization grids exhibited by each AGNR configuration. For smaller tensile uniaxial strain, $\varepsilon \ll 9\%$, a maximum energy gap opening of 0.62 eV is observed in $3m$ AGNR at 9% strain, which is comparable to 0.67 eV of Ge. It is worth noting that metallic $3m+2$ AGNR exhibits a phase transition to semiconductor

with the application of the strain. This phenomenon can be explained by the alteration of hopping integral t between the π-orbitals of AGNR and the weakest confinement that is responsible for the band split out from the Fermi level.[14,15,24] In addition, the edge bond relaxation significantly manipulates the energy curvature, which affects the band gap and the electron effective mass in the conduction band edge. For $N = 3m+2$, because of the linear dispersion relation, the effective mass cannot be cleared. A decrease of the electron effective mass in $3m$ AGNRs as a result of the edge bond relaxation has been reported; on the contrary, an amplified effective mass in $(3m+1)$ AGNRs has been observed in Refs. [21]–[23].

From the band structure, we can obtain the density of states (DOS). In the non-parabolic approximation, the DOS can be described as

$$\mathrm{DOS} = \frac{1}{2\pi\sqrt{B}} \cdot \frac{E}{\sqrt{E^2 - E_c^2}}. \tag{4}$$

The density of state is shown in Fig. 4.

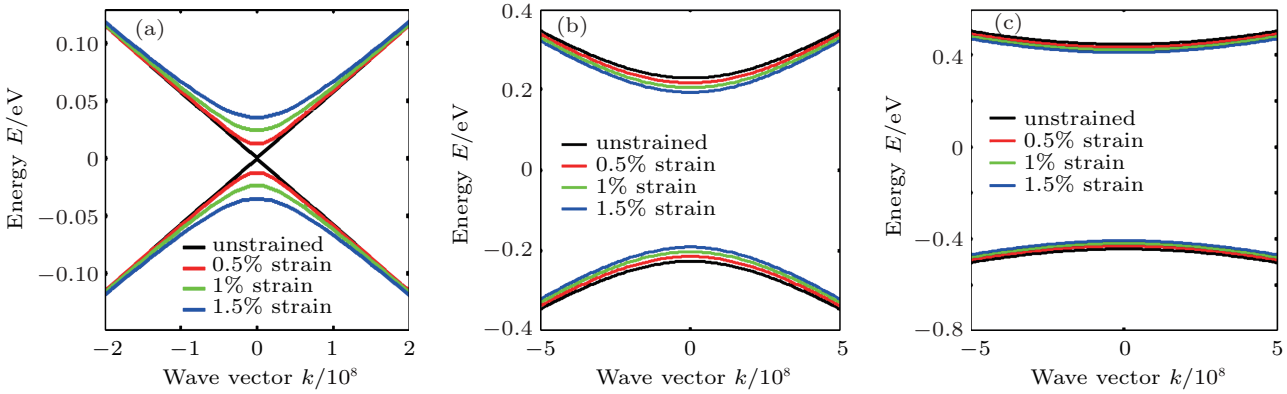


Fig. 3. (color online) The uniaxial strain effect on AGNR band structure for (a) $3m$ AGNR, (b) $3m+1$ AGNR, and (c) $3m+2$ AGNR, where $m = 6$ is a positive integer.

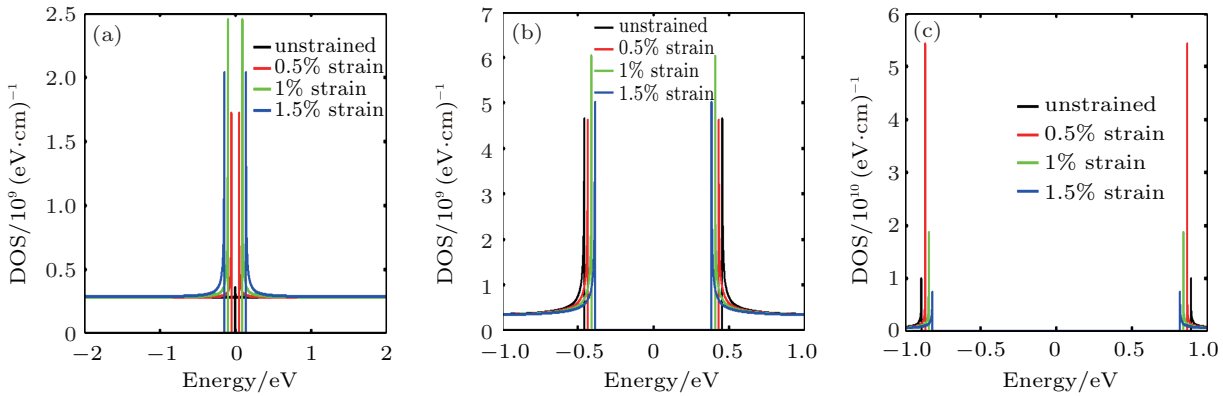


Fig. 4. (color online) The uniaxial strain effect on AGNR density of states near the Fermi level for (a) $3m$ AGNR, (b) $3m+1$ AGNR, and (c) $3m+2$ AGNR, with $m = 6$.

The densities of state for the three families of AGNRs are derived. From the results in Fig. 4, it can be seen that the energy dispersion relation gives rise to a DOS that varies as $E^{-1/2}$ for the one-dimensional strained AGNR. The number of states available to be occupied by carriers with distributed energy is represented by the Van Hove singularities at the band edge. In addition, the magnitude of gap is determined by the gap opening of DOS. Under tensile uniaxial strain, the number of states in the energy band of $3m$ AGNR (Fig. 4(a)) increases fairly with the increase of the energy band gap. However, the strained $3m+1$ AGNR (Fig. 4(b)) exhibits an excessively smaller DOS compared to the unstrained AGNR and varies irregularly upon strain. Surprisingly, despite having a phase transition, $3m+2$ AGNR has higher DOS at 9% strain as can be observed in Fig. 4(c).

Generally, the number of states influences the number of carriers in the system. The total carrier concentration in the non-parabolic band of strained AGNR is obtained by integrating the density of states DOS(E) and Fermi–Dirac distribution function $f(E)$ over energy as

$$n = \int \frac{1}{2\pi\sqrt{B}} \frac{E}{\sqrt{E^2 - E_c^2}} \frac{1}{1+\exp[(E-E_F)/k_BT]} \mathrm{d}E. \tag{5}$$

However, it is not in the form of a simple integral. Hence, the integral part is numerically solved as

$$n = N_c \int_{E_c}^{\infty} \frac{x + (E_c/k_BT)}{\sqrt{x^2 + 2E_c x/k_BT}} \cdot \frac{1}{1+\mathrm{e}^{x-\eta}} \mathrm{d}x, \tag{6}$$

where $x = (E - E_c)/k_B T$, $\eta = (E_F - E_c)/k_B T$, $dE = dx k_B T$, and $N_c = (\sqrt{k_B T})^3/2\pi\sqrt{B}$ is the effective density of states. In theory, the concentration of carriers is closely related to the Fermi level. The carriers are in the non-degenerate regime whenever the Fermi level lies more than $3k_B T$ away from either band edge, or else they are in the degenerate regime, as shown in Fig. 5.

The numerical integral is the most identical approach to describe the concentration of carriers in both regimes as shown in Fig. 5. In the non-degenerate regime, the temperature dependences are noticed as the distribution function is simplified into e^{η}, while the Fermi energy is strongly dependent on the carrier concentration in the degenerate regime. To observe the effect of strain on the AGNR carrier statistic, the numerical result is plotted in Fig. 6. As can be seen in Figs. 6(a) and 6(c), the amount of carriers increases in $3m$ AGNR and $3m+2$ AGNR when uniaxial strain is added. However, in $3m+1$ AGNR (Fig. 6(b)), it tends to decrease and increase with the amount of strain.

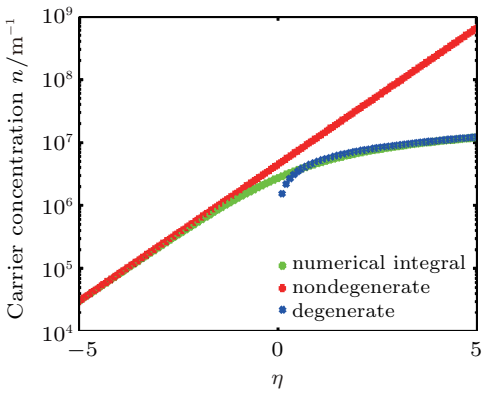


Fig. 5. (color online) The normal AGNR carrier concentration as a function of normalized Fermi energy η.

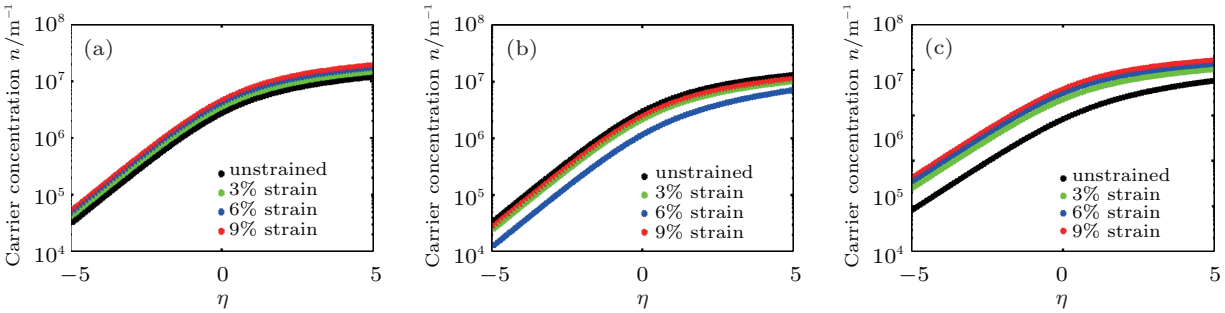


Fig. 6. (color online) The uniaxial strain effect on AGNR carrier concentration for (a) $3m$ AGNR, (b) $3m+1$ AGNR, and (c) $3m+2$ AGNR, with $m = 6$.

3. Conclusion

Because of the technological limit on conventional materials, researchers are engaged with new resources such as graphene. Graphene has a non-parabolic dispersion relation on its band structure which is highlighted in this study. Based on the non-parabolic energy band, the relation between the energy and the total number of allowed states in the conduction or valence band is investigated. The numerical result is obtained. Since the nano scale device operation regime is mainly the degenerate regime instead of the non-degenerate limit, therefore the concentrations of carriers in both regimes are modelled. Finally, the effect of strain on the AGNR carrier statistic is numerically explored and the amount of carriers is reported to be increased for $3m$ AGNR and $3m+2$ AGNR when uniaxial strain is added.

References

[1] Geim A K and Novoselov K S 2007 *Nat. Mater.* **6** 183

[2] Zhu Y, Murali S, Cai W, Li X, Suk J W, Potts J R and Ruoff R S 2010 *Adv. Mater.* **22** 3906

[3] Obeng Y and Srinivasan P 2011 *Interface-Electrochemical Society* **20** 47

[4] Tang C, Wei X L, Tan X, Peng X Y, Sun L Z and Zhong J X 2012 *Chin. Phys. B* **21** 066803

[5] Barone V, Hod O and Scuseria G E 2006 *Nano Lett.* **6** 2748

[6] Wang X, Ouyang Y, Li X, Wang H, Guo J and Dai H 2008 *Phys. Rev. Lett.* **100** 206803

[7] Deng S X and Liang S D 2012 *Chin. Phys. B* **21** 047306

[8] Son Y W, Cohen M L and Louie S G 2006 *Phys. Rev. Lett.* **97** 216803

[9] Wang Z F, Li Q, Zheng H, Ren H, Su H, Shi Q W and Chen J 2007 *Phys. Rev. B* **75** 113406

[10] Son Y W, Cohen M L and Louie S G 2006 *Phys. Rev. Lett.* **97** 216803

[11] Zhou B H, Duan Z G, Zhou B L and Zhou G H 2010 *Chin. Phys. B* **19** 037204

[12] Ungersboeck E, Dhar S, Karlowatz G, Sverdlov V, Kosina H and Selberherr S 2007 *IEEE Transactions on Electron Devices* **54** 2183

[13] Yang L, Anantram M P, Han J and Lu J P 1999 *Phys. Rev. B* **60** 13874

[14] Lu Y and Guo J 2010 *Nano Research* **3** 189

[15] Mei H, Yong Z and Hong-Bo Z 2010 *Chin. Phys. Lett.* **27** 037302

[16] Johari Z and Ismail R 2013 *Nanoscale Research Letters* **8** 479

[17] Levy N, Burke S A, Meaker K L, Panlasiqui M, Zettl A, Guinea F, Castro Neto A H and Crommie M F 2010 *Science* **329** 544

[18] Guinea F 2012 *Solid State Commun.* **152** 1437

[19] Ni G X, Yang H Z, Ji W, Baeck S J, Toh C T, Ahn J H, Pereira V M and Özyilmaz B 2014 *Adv. Mater.* **26** 1081

[20] Sun J T, Du S X, Xiao W D, Hu H, Zhang Y Y, Li G and Gao H J 2009 *Chin. Phys. B* **18** 3008

[21] Xu C, Li H and Banerjee K 2009 *IEEE Transactions on Electron Devices* **56** 1567

[22] Tsuchiya H, Ando H, Sawamoto S, Maegawa T, Hara T, Yao H and Ogawa M 2010 *IEEE Transactions on Electron Devices* **57** 406

[23] Sako R, Hosokawa H and Tsuchiya H 2011 *IEEE Electron Device Letters* **32** 6

[24] Han M Y, Özyilmaz B, Zhang Y and Kim P 2007 *Phys. Rev. Lett.* **98** 206805